This article has been accepted for publication in a future issue of this journal, but has not been fully edited. Content may change prior to final publication. Citation information: DOI 10.1109/TVT.2013.2287102, IEEE Transactions on Vehicular Technology

Energy Management for a Power-Split Plug-in Hybrid Electric Vehicle Based on Dynamic Programming and Neural Networks

Zheng Chen, *Member, IEEE*, Chunting Chris Mi, *Fellow, IEEE*, Jun Xu, *Student Member, IEEE*, Xianzhi Gong, and Chenwen You

***Abstract*—This paper focuses on building an efficient, online, and intelligent energy management controller to improve the fuel economy of a power-split plug-in hybrid electric vehicle (PHEV). Based on the detailed powertrain analysis, the battery current can be optimized to improve the fuel economy using dynamic programming (DP). Three types of drive cycles, highway, urban, and urban (congested), are classified and six typical drive cycles are analyzed and simulated in order to study all the driving conditions. An online intelligent energy management controller is built which consists of two neural network (NN) modules trained based on the optimized results obtained by DP method, considering the trip length and duration. Based on whether the trip length and duration is known or unknown, the controller will choose the corresponding NN module to output the effective battery current commands to realize the energy management. Numerical simulation shows that the proposed controller can improve the vehicle fuel economy.**

***Index Terms*—Battery, dynamic programming (DP), neural network (NN), plug-in hybrid electric vehicle (PHEV), state of charge (SOC), trip length and duration.**

I. Introduction

Hybrid and plug-in electric vehicles (HEVs/PHEVs) have excellent fuel economy and environmental advantages [1-6]. HEVs and PHEVs are powered with two drive trains, one or two electric motors and an internal combustion engine (ICE). Managing the proper propulsion energy distribution between the two drive trains [4, 5] becomes very essential and important. PHEVs, which are equipped with a larger energy storage system, represent the development trend of HEVs. Besides working under hybrid mode or charge-sustaining (CS) mode, PHEVs can power the vehicle by using only the stored energy charged from the power grid, referred to as charge depletion (CD) mode [7]. This is the major difference between a PHEV and a HEV. It combines the merits of a HEV and an electric vehicle (EV). Thus it is more important and more complicated to manage the energy distribution between the two drive trains for a PHEV than for a HEV. An appropriate energy management strategy can improve the fuel economy, decrease the operation cost, and prolong the battery life without sacrificing the driving performance. The target of this paper is to propose an online and intelligent controller to improve the fuel economy of a PHEV.

Since the PHEV has the capability of all electric driving (AER), the simplest way to manage the energy distribution between battery and ICE is to classify the vehicle running mode into two modes: CD mode and CS mode [7]. During CD mode, the vehicle can be powered mostly by electric motors until the battery state of charge (SOC) [8] drops to a preset low-threshold. After that, the vehicle changes into CS mode, under which the vehicle works like a conventional HEV, and maintains the SOC at the vicinity of the low-threshold. This control algorithm is simple and easy to implement. However, it may not save fuel consumption in either CD or CS modes, as the motor and ICE are only to satisfy the propulsion demand without considering efficiency optimization and may not work in the high efficiency region.

Substantial research efforts have been carried out on the energy management of HEV and PHEV to improve fuel economy [4-6, 9-28], prolong battery life [14, 23] with or without the help of global positioning system (GPS) or geographic information system (GIS) [29, 30]. The research methods can be classified into three categories: (1). Analytic methods [4, 5, 9, 31]; (2). Intelligent control algorithms such as fuzzy logic [13, 24], neural networks (NNs) [5, 11, 12, 22], and model predictive control methods (MPC) [25], genetic algorithms [10]; and (3). Optimal theory methods such as minimum theory [16, 19] and DP method [5, 11-13, 15, 20, 29, 32] which includes deterministic DP and stochastic DP. They will be briefly discussed below.

1) Analytic Method

This type of methods mainly focuses on the powertrain analysis and is based on several running modes of PHEV. In [9], an intelligent charge-depleting control strategies and fuel optimization for a blended-mode PHEV was proposed with known electric system loss characteristics, and other variables

The authors are with the Department of Electrical and Computer Engineering, University of Michigan-Dearborn, Dearborn, MI 48128 USA (e-mail: botaoc@gmail.com, chrismi@umich.edu, xujun018@gmail.com, xianzhigong@gmail.com, youc@umich.edu).

This article has been accepted for publication in a future issue of this journal, but has not been fully edited. Content may change prior to final publication. Citation information: DOI 10.1109/TVT.2013.2287102, IEEE Transactions on Vehicular Technology

but without the detailed trip information. The proposed method cannot give an optimal solution for the energy management with simple analysis. In [31], a modern analytical approach was proposed for the power management of blended-mode PHEVs. The power management strategy was represented by a pair of power parameters that describe the power threshold for turning on the engine as well as the optimum battery power in engine-on operations. The target is a blended-mode PHEV, and the method is not universal for all PHEVs which also include extended-range PHEVs.

2) Intelligent Method

In [5, 13, 24-26], several typical intelligent methods, such as fuzzy logic, MPC, and NNs, are used to control the energy distribution in a HEV or PHEV. In [24], the battery working state (BWS) was used by a fuzzy logic energy management system of a PHEV to make the decision on the power split ratio between the battery and the engine based on the BWS and vehicle power demand. The safety of the battery is of most importance in the paper. In [25], MPC-based energy management of a power-split HEV was introduced to obtain the power split between ICE and battery, whereas it did not consider the total trip length and full use of the battery.

3) Optimal Theory Method

Generally, optimal theory methods include the minimum theory and DP methods (including deterministic DP and stochastic DP). In [29, 30], a trip-based optimal energy management method was proposed for PHEV based on DP method. The proposed method needs the detailed trip information and needs too much calculation and computation time which decreases the feasibility of application of the method. In [32], a stochastic dynamic programming to optimize PHEV energy management was proposed with consideration of the fuel and electricity price. The method was based on a distribution of drive cycles and had the function of predicting road conditions. However, it still needs some considerable calculation which increases the calculation burden of the vehicle controller when applied online. Besides, it did not consider the whole trip length so that it may not use up all the available electric energy stored in the battery in a given trip. In [18], an intelligent multi-feature statistical approach to automatically discriminate the driving condition of the HEV was proposed and a support vector machine (SVM) method to intelligently and automatically discriminate the driving conditions was applied to classify the road pattern with high accuracy. It does not apply to a PHEV with a larger battery capacity. In [19], a model-based control approach for PHEV energy management to reduce the overall CO_2 emissions was introduced by applying the Pontryagin's minimum theory and considering the electricity constitution in different countries and areas under known trip information as a prior knowledge. A machine learning framework that combines DP and quadratic programming (QP) was proposed in [11, 12, 22]. The machine learning is to learn about roadway-type and traffic congestion level. They are only applied to HEV with a small range of SOC variation.

Based on the above discussion, a conclusion can be made that an intelligent controller with fast calculation and excellent control performance is necessary for a PHEV. Given the detailed or basic trip information such as trip length and trip duration, the fuel economy can be improved. This is the main motivation of this paper. In this paper, the main target is to improve the fuel economy of a PHEV with known trip information such as trip length and trip duration. We selected a power-split PHEV as the research object. The PHEV has two motors/generators, and is more complicated compared with a series or parallel PHEV. In order to build a fast, online, easy to implement, and effective energy management controller, we first applied an offline method, DP, to obtain the optimal energy distribution between ICE and battery by numerical calculations considering different road types. Then, based on the optimized results, NN is introduced to train them to generate an online optimal energy controller with known trip length and trip duration.

The NN controller [11, 12, 22] includes a variety of formulas to store the optimal energy distribution information based on vehicle speed, acceleration/deceleration, trip information including trip length and duration, and battery SOC. In order to build an effective NN controller, abundant vehicle simulation data based on DP method are essential which can include all driving conditions. In this paper, six standard drive cycles are used to simulate the vehicle operating condition, including Urban Dynamometer Driving Schedule (UDDS), SC03, Highway Fuel Economy Driving Schedule (HWFET), US06_HWY, Manhattan (MANN) and New York City Cycle (NYCC), which can represent the criterions of highway, urban and urban congested driving conditions to test the light duty vehicle in the United States. Each drive cycle is simulated with multi consecutive iterations to consider enough driving distances and durations.

Then, we applied the controller to drive scenarios with unknown trip information. It was shown that the proposed method can still save fuel consumption even without knowing the trip length or duration although the benefits is significantly reduced.

II. Vehicle Model and Analysis

The objective in the paper is to optimize the fuel consumption of a power-split PHEV during a certain trip, which can be expressed as an optimization problem:

$$\min F = \min \sum_{t=0}^{t=n} m_f(t,v) \tag{1}$$

where F is the total fuel consumption, n is the trip duration, and m_f is the fuel rate determined by engine speed w_e and engine torque T_e,

$$m_f = f(T_e, w_e) \tag{2}$$

where f is a high nonlinear function.

This article has been accepted for publication in a future issue of this journal, but has not been fully edited. Content may change prior to final publication. Citation information: DOI 10.1109/TVT.2013.2287102, IEEE Transactions on Vehicular Technology

In order to calculate m_f and optimize F, the vehicle powertrain should be analyzed in detail. The powertrain structure of the power-split PHEV analyzed in the paper is shown in Fig. 1. The vehicle includes a gasoline ICE, two electric motors, a lithium-ion battery pack, and a planetary gear set, which combines engine, motor and the final driveline together with a particular gear ratio [5, 10-13].

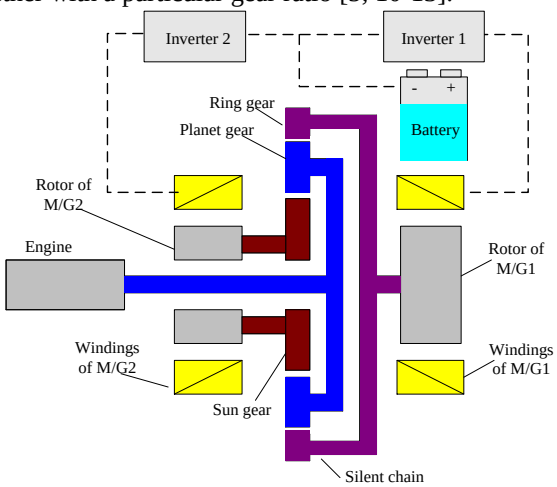

Fig. 1. Power-split vehicle powertrain.

From Fig. 1, the vehicle can be powered by the motor only, the engine only, or both [5]. There exist several modes according to the power flow [10, 13], and it increases the analysis complexity of fuel rate. The vehicle driveline power P_o equals the sum of ring power P_r and motor 1 power P_{mot1}, i.e.,

$$P_o = T_o w_o = P_r + P_{mot1} = T_r w_r + T_{mot1} w_{mot1} \tag{3}$$

where T_o, T_r, and T_{mot1} denote the torque of driveline, ring gear of the planetary gear set and motor 1, w_o, w_r, and w_{mot1} denote their speeds respectively. The driveline torque T_o should satisfy

$$\begin{cases} T_o = (T_r + T_{mot1} r_{mot1}) \cdot r_{final} \\ w_{mot1} = w_o / (r_{final} r_{mot1}) \\ w_r = w_o / r_{final} \end{cases} \tag{4}$$

where r_{mot1} and r_{final} are the gear ratio between motor 1 and driveline, driveline and vehicle wheels, respectively. The planetary gear set consists of a sun gear, a ring gear and carrier, which connects motor 2, driveline, and engine respectively. Neglecting the friction and inertia losses, there are two basic equations for speed and torque of the planetary gear set,

$$\begin{cases} (1+\rho) \cdot w_e = \rho \cdot w_{mot2} + w_r \\ T_e = (1 + 1/\rho) \cdot T_{mot2} = (1+\rho) \cdot T_r \end{cases} \tag{5}$$

where ρ is the ratio of sun gear and ring gear, w_e, w_{mot2} represent the speed of engine, motor 2, and T_e and T_{mot2} are their torques. Based on (3) to (5), we can calculate T_e further:

$$T_e = \frac{1}{1+\rho} \cdot \frac{T_o - P_b \cdot \eta_{mot1}}{r_{final} w_o} + \frac{1}{(1+\rho)^2} \cdot \frac{((1+\rho) \cdot w_e - r_{final} w_o)}{r_{final} w_o} \cdot \frac{\eta_{mot1}}{\eta_{mot2}} \cdot T_e \tag{6}$$

where η_{mot1} and η_{mot2} are motor 1 and motor 2 efficiency, P_b and P_{mot2} are the battery and motor 2 power. Solving (6), we can get

$$T_e = \frac{\dfrac{1}{1+\rho} \cdot \dfrac{T_o - P_b \cdot \eta_{mot1}}{r_{final} w_o}}{1 - \dfrac{1}{(1+\rho)^2} \cdot \dfrac{((1+\rho) \cdot w_e - r_{final} w_o)}{r_{final} w_o} \cdot \dfrac{\eta_{mot1}}{\eta_{mot2}}} = g(T_o, P_b, w_o, w_e) \cdot \tag{7}$$

From (7), T_e can be determined by T_o, P_b, w_o, and w_e. As T_o and w_o are determined to satisfy the vehicle torque demand, and cannot be influenced by control algorithms, T_e can be controlled by different w_e and P_b. P_b can be approximately calculated by battery current I, battery open circuit voltage V_{ocv} and battery internal resistance R [10-12],

$$P_b = V_{ocv} I + I^2 R. \tag{8}$$

Hence, equation (2) can be changed into

$$m_f = f(T_e, w_e) = f_{new}(I, w_e). \tag{9}$$

Now we can see that w_e and I can influence the fuel rate, and therefore can be optimized to minimize the fuel consumption for a given trip. The calculation process includes some nonlinear efficiency coefficients, such as η_{mot1}, η_{mot2}, and fuel rate function f, which makes it not realistic to solve m_f based on (3) to (9). Therefore, Pontryagin's Minimum principle [16, 19] is not appropriate for the optimization of fuel consumption. It needs to build a deterministic relationship between the input and the output, construct a Hamiltonian function, consider a proper boundary for each variable and solve the partial differential function. DP [11, 12, 21, 33] does not need to get a detailed numerical solution, can easily apply the constraint of each variable, and can be easily applied in the discrete system. Based on the above discussion, we use DP to solve the energy management problem.

III. Dynamic Programming

DP is a numerical technique which can be applied to any problem that requires decisions to be made in stages with the objective of finding a minimal penalty decision pathway [5, 11-13, 20, 21]. DP combines knowledge of the immediate penalty of the decision at hand with knowledge of future penalties that arise as a result of the immediate decision. DP is commonly used for global optimization of the energy management of hybrid electric vehicles [11-13, 20]. Generally, it needs to define the constraints of each variable used to realize DP algorithm and the grid size which can determine the calculation precision and time consumption.

As discussed in Section II, the battery current I and engine speed w_e influence the fuel rate, and can be regarded as the controlled variables to realize DP algorithm. However, it

This article has been accepted for publication in a future issue of this journal, but has not been fully edited. Content may change prior to final publication. Citation information: DOI 10.1109/TVT.2013.2287102, IEEE Transactions on Vehicular Technology

induces two degrees of freedom of optimization, which brings too much computation and high calculation cost [11, 12]. In order to simplify the calculation without influencing the precision, a method is proposed to convert the two degrees of freedom problem into a one degree of freedom problem. For each operating point, we can find out the optimal operating efficiency point according to different engine power. This way, at each engine operating power, we can determine the optimal engine speed w_e accordingly. It means that the engine can only work in the highest efficiency region at different power levels, and the fuel rate can only be determined by engine torque T_e. Fig. 2 shows the relationship between the engine power P_e and speed w_e with a 1kW increment for the next step. Based on this relationship, we can easily find the relationship between w_e and T_e,

$$w_e = g_1(T_e)\,. \tag{10}$$

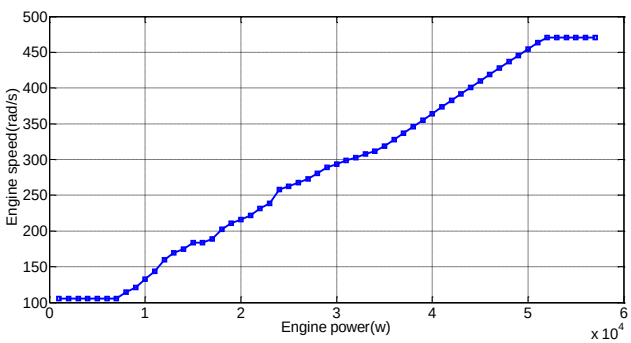

Fig. 2. The optimal speed profile at different engine power output.

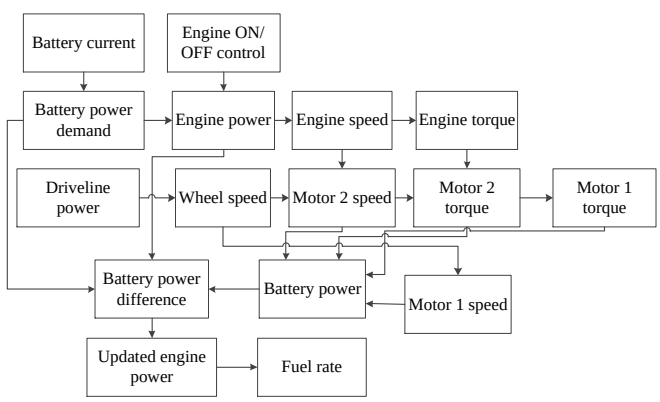

Fig. 3. The calculation process.

Now based on (7) to (10), we can solve the fuel rate based on battery current I only. With different I commands, the motor power can be determined accordingly, and the engine power and engine fuel rate can be calculated. As presented in (6) to (9), we need to know the motor efficiency and fuel rate relationship when calculating the fuel rate which cannot be obtained directly. Here, we use distributed computing method to get the fuel rate from battery current. Equation (11) to (21) detail the calculation and Fig. 3 shows the calculation process. First, motor 1 speed can be determined by the vehicle speed,

$$w_{mot1} = w_{ring} = \frac{v_s}{wheel\_r} \times r_{final} \tag{11}$$

where $wheel\_r$ is the wheel radius, and v_s is the vehicle speed.

Based on different I, we can calculate the temporary engine power,

$$P_e^* = P_{drive} + P_b + P_L = V_{ocv} I + I^2 R + P_o + P_L \tag{12}$$

where P_L is the accessory power of the vehicle, P_e^* is the temporary engine power. According to the relationship in (10), the speed and torque of engine and motor 2 can be calculated,

$$w_{mot2} = w_e(1+\frac{1}{\rho}) - w_{mot1}\frac{1}{\rho} \tag{13}$$

$$T_{mot2} = \frac{\rho}{\rho+1} T_e^* \tag{14}$$

where T_e^* is the temporary engine torque. Based on engine torque, we can calculate the ring torque and motor 1 torque accordingly,

$$T_{ring} = \frac{1}{1+\rho} T_e^* \tag{15}$$

$$\begin{aligned} P_o &= P_{mot1} + P_{ring} \\ &= T_{ring} w_{ring} + T_{mot1}\omega_{mot1} = (T_{ring} + T_{mot1})\omega_{mot1} \end{aligned} \tag{16}$$

$$T_{mot1} = P_o / w_{mot1} - T_{ring}\,. \tag{17}$$

We have already known the motor speed and torque, thus the motor efficiency and losses can be determined:

$$\begin{cases} P_{mot1\_loss} = (1-\eta_{mot1}) T_{mot1} w_{mot1} \\ P_{mot2\_loss} = (1-\eta_{mot2}) T_{mot2} w_{mot2} \end{cases} \tag{18}$$

where η_{mot1} and η_{mot2} are motor 1 and motor 2 efficiencies. The updated engine power and torque can be obtained by the sum of temporary engine power and motor losses,

$$\begin{aligned} P_e &= P_e^* + P_{mot1\_loss} + P_{mot2\_loss} \\ &= P_o + P_b + P_L + P_{mot1\_loss} + P_{mot2\_loss} \\ &= V_{ocv} I + I^2 R + P_L + P_o + P_{mot1\_loss} + P_{mot2\_loss} \end{aligned} \tag{19}$$

Based on the new engine power P_e, the engine torque T_e and engine speed w_e can be determined by (10) and finally the updated engine fuel rate can be calculated. It is worth to point out that the motor speed and torque may vary with the new engine speed and torque, we assume their efficiency keep unchanged during the calculation.

$$\tau_{eng} = P_{eng} / w_{eng} \tag{20}$$

$$f(w_{eng}, \tau_{eng}) = f_{new2}(I)\,. \tag{21}$$

In order to realize DP, some constraints [11, 12, 21] should be considered, such as engine maximum power, engine maximum and minimum speed, battery maximum charge and discharge current, motor maximum and minimum power:

This article has been accepted for publication in a future issue of this journal, but has not been fully edited. Content may change prior to final publication. Citation information: DOI 10.1109/TVT.2013.2287102, IEEE Transactions on Vehicular Technology

$$\begin{cases} 0 \le P_e \le P_{\max}, w_{\min} \le w_e \le w_{\max} \\ P_{mot1\_\min} \le P_{mot1} \le P_{mot1\_\max} \\ P_{mot2\_\min} \le P_{mot2} \le P_{mot2\_\max} \\ P_{b\_\min} \le P_b \le P_{b\_\max} \\ C_{b\_\min} \le C_b \le C_{b\_\max} \end{cases} \quad (22)$$

where the subscript "min" and "max" denote the minimum and maximum value of each variable, and C_b is the battery capacity in Ampere-seconds (As). In order to realize DP, a cost-to-go matrix should be built, in which some variables, such as time interval Δt, total length t_{total} and grid size ΔC_b should be determined.

Due to the bounds of energy, certain grid levels between $C_{b\_\min}$ and $C_{b\_\max}$ needs to be determined [5, 20]. This area is mapped onto a fixed grid with determined distance ΔC_b, so that $m+1$ capacity levels are considered.

$$m = \left\lfloor \frac{C_{b\_\max} - C_{b\_\min}}{\Delta C_b} \right\rfloor. \quad (23)$$

The optimal values are calculated afterwards, by starting at $C_b(n)$ (n is the duration of drive cycle) and then following the path of minimal cost. Given the sequence of I, the requested set-points for the motor and generator are found. All calculations required for DP can be done in a reasonable amount of time due to the simple dynamics and all the restrictions of I, C_b, w_e, P_{mot1}, P_{mot2} and P_e. However, the computation increases rapidly with the driving cycle length and the grid density [20], especially when we apply several consecutive drive cycles. Considering the computation complexity and precision, we set $\Delta t = 1s$.

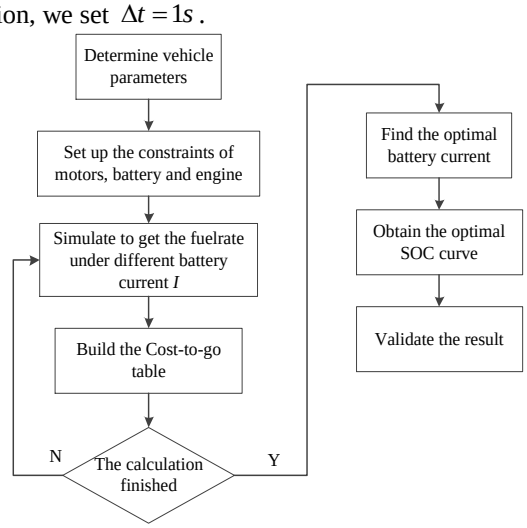

Fig. 4. The procedure of realizing DP method.

The steps to realize DP is shown in Fig. 4. First, the constraints of motors, battery and engine should be considered properly, and the engine fuel rate can be calculated according to (11) – (21) with different battery current. At the same time, the cost-to-go matrix can be built. After getting the cost-to-go matrix, the optimal SOC curves and optimal battery current with different beginning SOCs can be obtained. The last step is to validate the result as we missed some issues, such as inertia of motors and engine, and simplified some variables during the calculations. Table I lists the vehicle parameters.

TABLE I
VEHICLE PARAMETERS

Vehicle type	Plug-in split HEV
Vehicle mass	1641.3kg
Engine power	57kW
Motor power	25kW, peak power 50kW
Generator power	15kW, peak power 30kW
Planetary gear set	Sun gear 30 Ring gear 78
Battery	Lithium-ion battery Rated capacity 20Ah Rated voltage 356V

IV. DP RESULT: ANALYSIS AND APPLICATION

We need to validate the DP results through simulation and analysis. Due to the high nonlinearity of the vehicle system, it is difficult to get the optimal result by approximating it to a linear or quadratic system. If we can simulate the vehicle with a constant speed profile, we can simplify the problem and analyze the result using the linear programming (LP) method to prove the correctness of DP result. Here, the whole validation is divided into two parts: (1). Constant speed simulation; and (2). Drive cycle simulation. Before analyzing the fuel consumption, the default control algorithm, i.e. CD and CS strategy, is applied to simulate and obtain the vehicle performance as a reference [7]. Considering the calculation cost, the current grid is set to 14.4A. According to the constraints of the battery, the current grid matrix can be built as follows.

$$I = [-100.8, -86.4, -72.0, -57.6, -43.2, -28.8, -14.4, 0, 14.4, 28.8, 43.2, 57.6, 72.0, 86.4, 100.8]. \quad (24)$$

At each step, the optimal battery current command can be selected from (24) to minimize the fuel consumption.

A. Constant Speed Simulation

We built the drive cycles with a constant speed driving time at 3600s and the vehicle is at rest for 50s at the beginning and ending time periods. The acceleration is 1mph/s in the beginning after rest time, and the deceleration is -1mph/s after the constant speed driving. So the total time of 50mph drive cycle equals 3800s. The vehicle driveline power demand during the whole drive cycle is shown in Fig. 5. The maximum power is 22.84kW and the constant power is 7.04kW when the vehicle speed stabilizes at 50mph.

The optimized battery current based on DP method is shown in Fig. 6. From 100s to 3700s, the battery is discharged with 14.4A current for 3511s and followed by 28.8A current for 89s. During this period, as the vehicle power demand is unchanged, it is easy to apply the analytical method to validate the DP result. The driveline power is 7.04kW, and if the vehicle can be driven by the battery only, the current is about 30A. So the available battery current range becomes:

This article has been accepted for publication in a future issue of this journal, but has not been fully edited. Content may change prior to final publication. Citation information: DOI 10.1109/TVT.2013.2287102, IEEE Transactions on Vehicular Technology

$$I = [-28.8, -14.4, 0, 14.4, 28.8, 43.2, 57.6, 72.0, 86.4, 100.8] \quad (25)$$

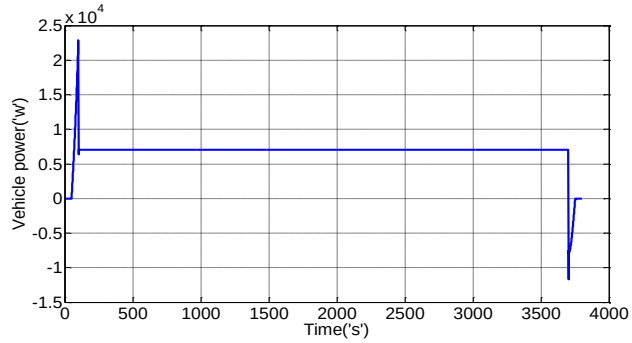

Fig. 5. Power demand of 50mph constant speed drive cycle.

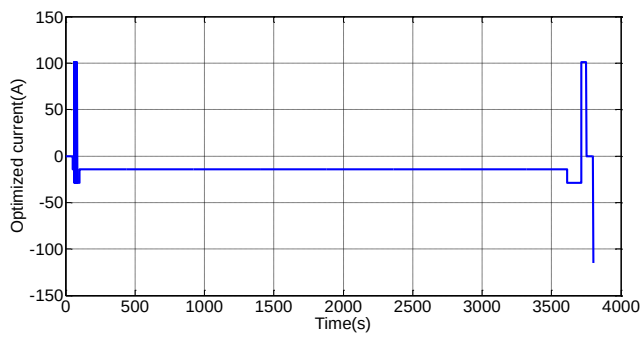

Fig. 6. Battery current obtained by DP method.

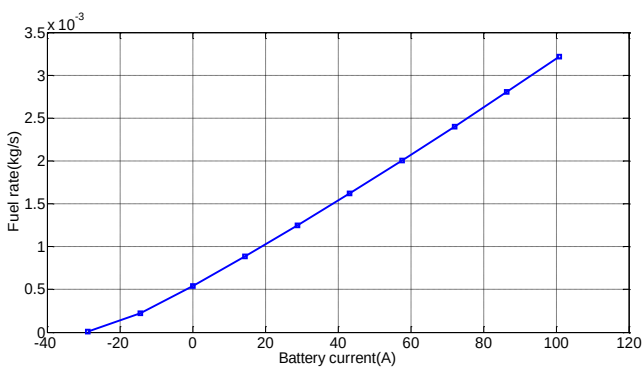

Fig. 7. Fuel rate for the 50mph constant speed drive cycle.

Fig. 7 shows the fuel rates with different battery currents according to (11) to (21), and they range from 0.00001kg/s to 0.00322kg/s. We implemented the LP method [34] to validate the DP result. From (25), as there are only 10 selections, we can calculate the following equations to get the optimal value,

$$F = Min(a_1 \cdot x_1 + a_2 \cdot x_2 + a_3 \cdot x_3 + ... + a_9 \cdot x_9 + a_{10} \cdot x_{10})$$

$$\begin{cases} \sum_{i=1}^{10} x_i = 3600 \\ -28.8 \cdot x_1 - 14.4 \cdot x_2 + 0 \cdot x_3 + 14.4 \cdot x_4 + \cdots + 100.8 \cdot x_{10} = \Delta soc \cdot C_b \\ x_i \geq 0, (\mathrm{i} = 1, 2, \cdots, 10) \\ x_i \in Integers \end{cases} \quad (26)$$

where $x_i (\mathrm{i} = 1, 2, \cdots, 10)$ denotes the duration time for each current state of (25), and are integers, and should be not less than 0. The sum of $x_i (\mathrm{i} = 1, 2, \cdots, 10)$ should equal 3600. $a_1, ..., a_{10}$ are fuel rates shown in Fig. 7, C_b equals 72000, Δsoc is the SOC range from 100s to 3700s, and equals 0.7378. Using LP method, the solution can be easily obtained,

$$\begin{cases} x_1 = 89 \\ x_2 = 3511 \\ x_3 = x_4 = x_5 = x_6 = x_7 = x_8 = x_9 = x_{10} = 0 \end{cases} \quad (27)$$

The result shown in (27) is identical as the result shown in Fig. 6. Therefore the DP result is turned out to be correct by LP method. However, LP method can only be used to analyze the constant vehicle power optimization, and cannot be used for the energy management for PHEV as the vehicle speed and power possibly change at all times.

It is necessary to use the SOC correction method to update the fuel consumption in order to compare the fuel saving at the same SOC. The linear regression method can be used to ensure that the initial and final SOCs are the same. Linear fitting method was adopted to obtain fuel consumption and corrected with SOC [9, 31]. Table II shows the results with different constant speed drive cycles. We can see that when the vehicle speed is at constant speed of 40, 50, and 60 mph, DP method can save 4.24%, 3.51%, and 1.16% of fuel. This way it shows the effectiveness of the DP method. But for 30 mph and 70 mph constant speed, DP does not show fuel savings. For 30mph drive cycle, when the default algorithm is applied, the engine is off all the time, and the vehicle is powered by the battery only. However, when the DP method is applied, engine starts during the acceleration period, which induces some fuel consumption. For 70mph drive cycle, when the default algorithm is applied, the engine and motors work in the high efficiency region, and their speeds keep unchanged. However, when the DP method is applied, the variation of battery current commands can make the motors and engine accelerate or decelerate, which costs more fuel consumption. Hence the proposed algorithm is more suitable for drive speed between 30 and 70 mph. In real world driving, constant speed driving rarely happens. Therefore, we predict that the proposed DP algorithm can help save fuel as long as the vehicle is driven mostly between 30 and 70 mph. This is also validated through real world driving cycle simulations in the next section.

This article has been accepted for publication in a future issue of this journal, but has not been fully edited. Content may change prior to final publication. Citation information: DOI 10.1109/TVT.2013.2287102, IEEE Transactions on Vehicular Technology

TABLE II
CONSTANT SPEED DRIVE CYCLE RESULT COMPARISON

Vehicle speed (mph)	Trip length (mile)	Duration (s)	Ending SOC (%)		Fuel consumption (kg)		Fuel savings (%)
			Default	DP	Default	DP (SOC corrected)	
30	30.26	3760	56.44	56.53	-	0.0016	-
40	40.46	3780	31.94	29.76	0.118	0.113	4.24
50	50.71	3800	32.21	30.68	1.083	1.045	3.51
60	61.02	3820	32.44	30.92	2.164	2.139	1.16
70	71.38	3840	32.63	31.08	3.503	3.546	-1.23

B. Drive Cycle Simulation

Several typical drive cycles are introduced to validate the DP algorithm. UDDS, also called "LA4" or "the city test", and SC03 drive cycles represent city driving conditions. HWFET and US06_HWY drive cycles represent highway driving conditions. NYCC and MANN drive cycles represent the congested city drive cycles [18]. Fig. 8 shows two of these six drive cycles. Table III presents total length, duration, maximum speed and average speed for each drive cycle. It needs to mention that as the NYCC and MANN cycle length is very short, we repeated them three times as new drive cycles.

TABLE III
DRIVE CYCLE COMPARISON

Type	Drive cycle	Length (miles)	Duration (s)	Maximum speed (mph)	Average speed (mph)
Freeway	HWFET	10.26	765	59.9	48.30
	US06_HWY	6.24	368	80.3	61.00
Urban	UDDS	7.45	1369	56.7	19.59
	SC03	3.60	596	54.8	21.60
Urban congested	3 NYCC	3.54	1794	27.7	7.10
	3 MANN	6.21	3267	25.4	6.80

In order to compare the results, the default algorithm, i.e. CD and CS method, were applied in the simulation to get the fuel consumption under different drive cycles. During CD mode, the vehicle is powered by the battery only. When the SOC drops near 30%, the vehicle is powered by the battery and engine together, which makes the battery SOC maintain at the low-preset threshold. The battery power is detailed in (28),

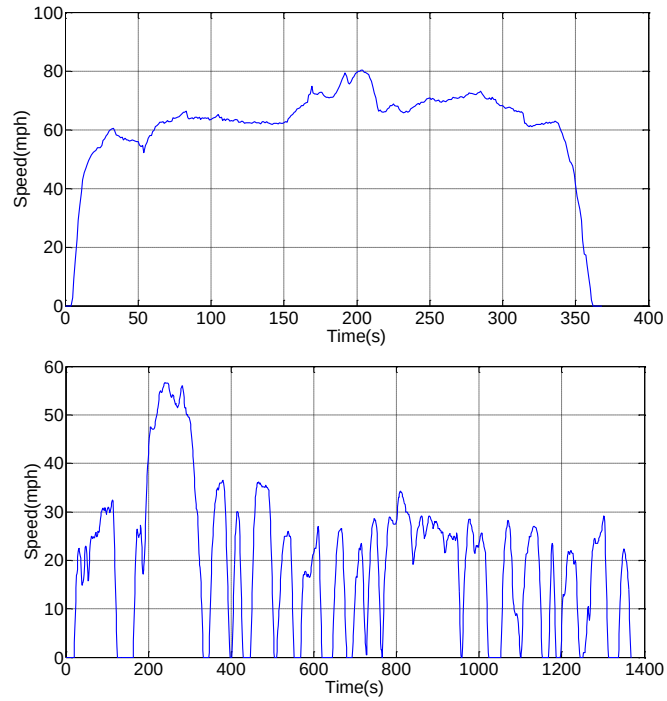

Fig. 8. Highway and urban drive cycles.

$$P_b = \begin{cases} P_o & SOC > 36\% \\ \min(31647, P_o) & 33\% \le SOC < 36\% \\ \min(31647 \cdot (SOC - 0.3)/0.03, P_o) & 30\% \le SOC < 33\% \\ \max(-30717 \cdot (SOC - 0.3)/0.03, P_o) & P_o < 0,\ 27\% \le SOC < 30\% \\ \max(-30717 \cdot (SOC - 0.3)/0.03, P_o - P_{e\_\max}) & P_o > 0,\ 27\% \le SOC < 30\% \\ \max(-30717, P_o) & P_o < 0,\ SOC < 27\% \\ \max(-30717, P_o - P_{e\_\max}) & P_o > 0,\ SOC < 27\% \end{cases} \tag{28}$$

TABLE IV
THE FUEL CONSUMPTION BASED ON CD/CS STRATEGY

Cycle Name	UDDS					HWFET					
No. of cycles	5	6	7	8	9	4	5	6	7	8	9
Distance (miles)	37.22	44.66	52.10	59.54	66.98	41.02	51.28	61.53	71.79	82.04	92.30
Fuel consumption (kg)	0.314	0.668	0.926	1.183	1.450	0.756	1.200	1.645	2.089	2.542	3.004

This article has been accepted for publication in a future issue of this journal, but has not been fully edited. Content may change prior to final publication. Citation information: DOI 10.1109/TVT.2013.2287102, IEEE Transactions on Vehicular Technology

where min( ) and max( ) denotes the minimum and maximum value of the two values given in the parenthesis, and $P_{e\_\max}$ is the maximum engine power. The engine's output should satisfy the demand of driveline power and battery power.

The initial battery SOC is supposed to be 100%. Figs. 9-10 show the battery SOC variation and engine fuel rates under UDDS driving cycle test. Before 5300s, the engine is off and the vehicle is powered by the battery and motors. When the battery SOC decreases to 30%, the engine starts and the vehicle works in CS mode, and the battery SOC maintains at the vicinity of 30%.

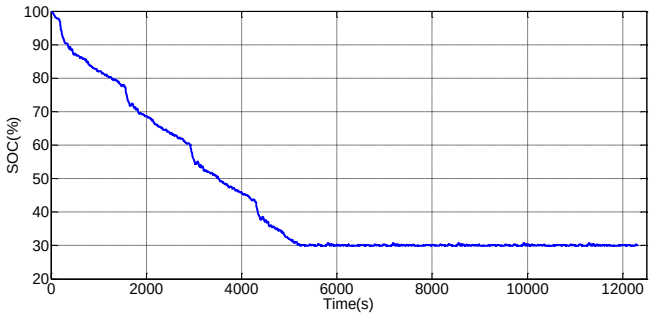

Fig. 9. Battery SOC variation.

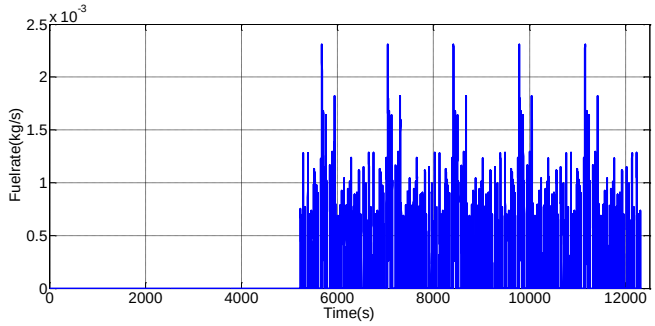

Fig. 10. Engine fuel rate.

The fuel consumptions under UDDS and HWFET drive cycles are listed in Table IV. Fig. 11 show the optimal SOC curves with different beginning SOC values under nine US06_HWY drive cycles, and five UDDS drive cycles. In Fig. 11, the beginning SOC is from 100% to 30% with 10% decrement for the next step. Fig. 12 compares the total fuel consumptions with different drive cycles, in which the fuel savings are 0.30%, 4.12%, 3.94%, 3.82%, 3.86%, and 3.77% with four to nine US06_HWY drive cycles, range from 12.63% to 2.85% with four to nine HWFET drive cycles, and from 14.91% to 4.92% with five to nine UDDS drive cycles respectively.

Fig. 13 compares the difference of the battery current in eight consecutive UDDS drive cycles when the different algorithms are applied. We can see that with the default algorithm, the battery is discharged more quickly than with DP method. Fig. 14 compares the engine efficiencies based on different algorithms. It can be seen that when the DP method is applied, the engine average efficiency is higher than that when the default algorithm is applied. To some extent, the comparisons can explain why DP method can save fuel consumption.

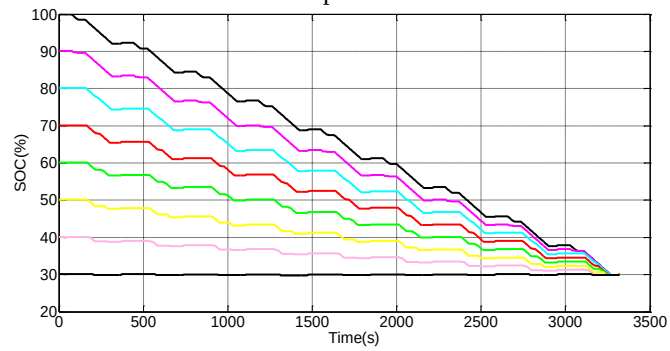

(a)

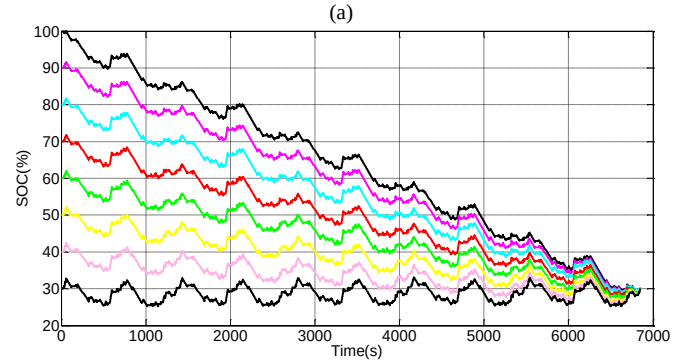

(b)

Fig. 11. Optimal SOC curve. (a). The optimal SOC curve based on nine consecutive US06_HWY drive cycles. (b). The optimal SOC curve based on five consecutive UDDS drive cycles.

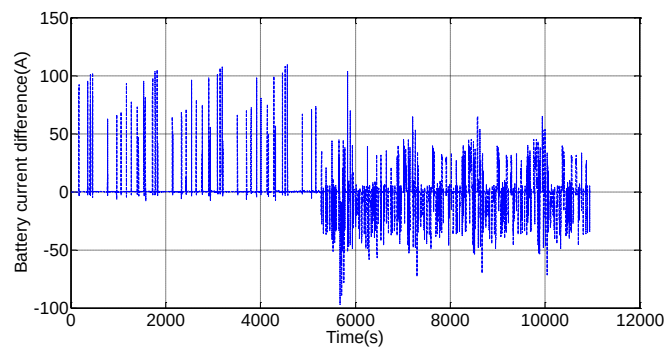

Fig. 13. Current difference.

This article has been accepted for publication in a future issue of this journal, but has not been fully edited. Content may change prior to final publication. Citation information: DOI 10.1109/TVT.2013.2287102, IEEE Transactions on Vehicular Technology

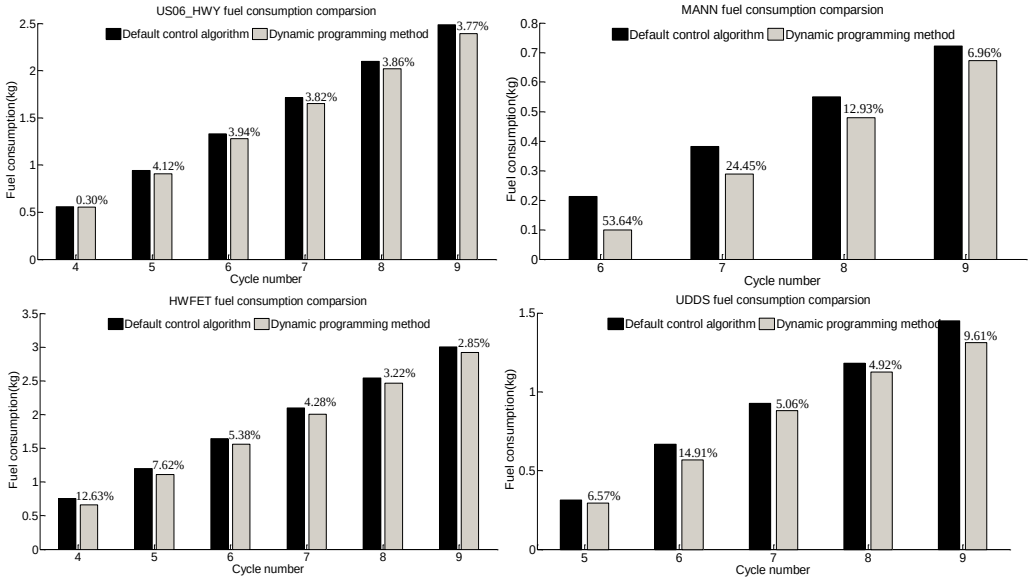

Fig. 12. Fuel consumption comparison under US06_HWY, MANN, HWFET and UDDS drive cycles.

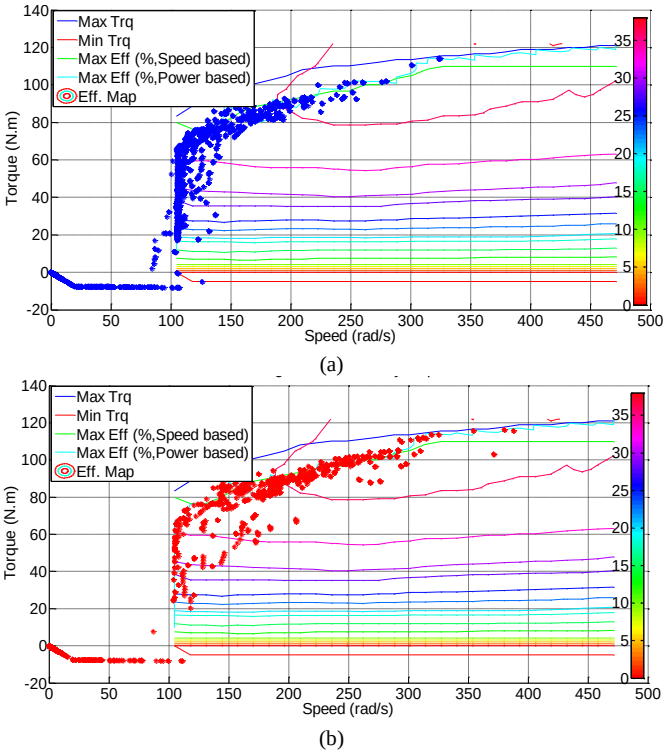

Fig. 14. Engine operating efficiency map. (a) Based on CS+CD algorithm. (b). Based on DP method.

V. Neural Network Training

As shown above, the DP result can improve fuel economy on conditions that the detailed trip information is known in advance. Besides, it also needs a large amount of computation. These limit the real-time application of DP algorithm. However, the optimal battery SOC and battery current values obtained by DP method can be regarded as a benchmark for further study. It is necessary to construct an online and effective controller based on the DP result to realize real-time control. It is difficult to get a deterministic equation or relationship as the energy management strategy is influenced by many factors, such as acceleration, speed, battery SOC, trip length, and trip duration, etc. NN can effectively learn the nonlinear relationship based on the optimized results and can generate an online controller to manage the energy distribution. Here, we apply NN to build an intelligent online controller to control the battery current, and consequently the engine torque and speed to improve the fuel economy. The controller, as shown in Fig. 15, consists of two NN modules, N1 and module N2 as shown in Fig. 16 and Fig. 17, respectively. The major difference between N1 and N2 is that N1 needs the trip information, i.e., trip duration and trip length. The principle of the controller is detailed in the following steps.

1) The beginning SOC is more than 30% and the trip length and trip duration is known or estimated before the trip starts. In this case, if the trip length is less than AER according to calculation based on the beginning SOC, the controller will adopt CD strategy and use the energy stored in the battery. Otherwise, the controller will select N1 as the controller to output the battery current commands to control the engine accordingly.

2) The beginning SOC is more than 30% and the trip information is unknown. In this case, the controller will use the electric energy until the SOC drops to 30%. Then the controller will select N2 to output the battery current command.

3) If the beginning SOC is not more than 30%, the controller will select N2 to output the battery current directly.

This article has been accepted for publication in a future issue of this journal, but has not been fully edited. Content may change prior to final publication. Citation information: DOI 10.1109/TVT.2013.2287102, IEEE Transactions on Vehicular Technology

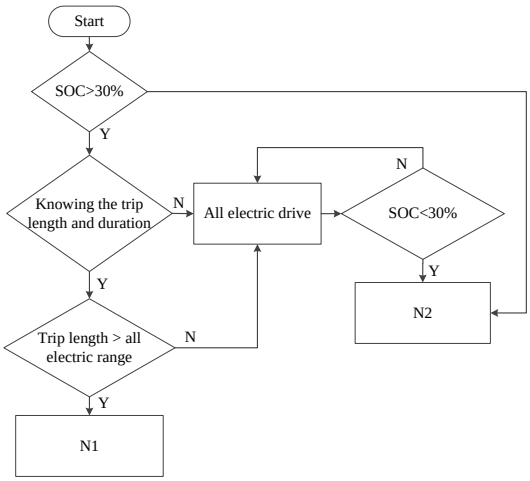

Fig. 15. Vehicle controller.

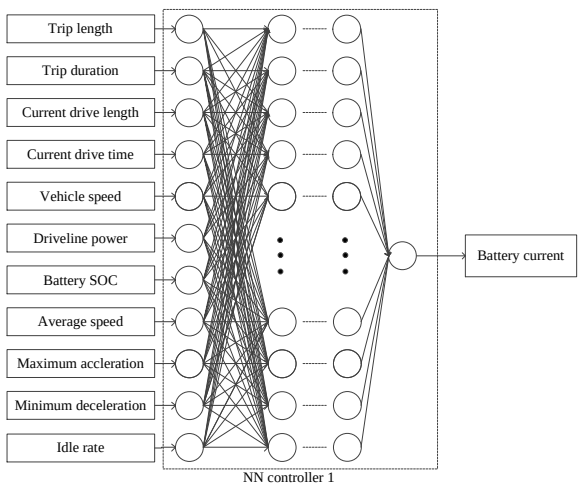

Fig. 16. NN controller N1.

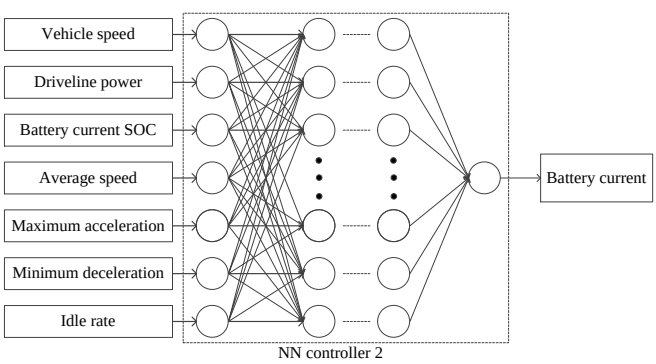

Fig. 17. NN controller N2.

The function of N1 is to output the battery current command based on the basic trip information. It needs the total trip length and trip duration in advance. Therefore, it contains at least four variables, trip length, trip duration, current drive length, and current drive time. In [11, 12, 22], the vehicle speed, driveline power, battery SOC, together with driving trend are utilized to train the NN to output the optimal battery power for a conventional HEV. Besides, the authors also employed another NN module to predict the road pattern based on eleven variables, which brings too much complexity. In [18], four variables, i.e., average speed, idle rate, maximum acceleration and minimum acceleration over a certain time interval, are applied to classify the driving patterns, of which the idle rate is the ratio of vehicle idle time during a certain time range. We combine them and select vehicle speed, driveline power, battery SOC, average speed, idle rate, maximum acceleration and minimum acceleration to train the controller to ensure the system precision. Therefore, N1 totally consists of the above mentioned eleven variables. Compared with [11, 12, 22], the energy management strategy proposed in this paper is easier to apply for energy management of a PHEV. During simulation, the time interval for calculating the average speed, the maximum acceleration, the minimum acceleration and the idle rate is 50s, 50s, 50s, and 100s respectively. The output of N1 is the battery current command. The beginning SOC to train the N1 is from 100% to 40% with 10% decrement for next step. We select the total drive cycle data including UDDS, HWFET, US06_HWY, SC03, NYCC and MANN cycles trained to generate N1.

Compared to N1, N2 does not consider the trip information, and is with only 7 inputs, which are vehicle speed, vehicle driveline power, battery SOC, average speed, idle rate, maximum acceleration and minimum acceleration. The beginning SOC of N2 is 30%. The output is the same as N1. The NN training performance is measured by mean squared errors (MSEs) E_{MSE} as shown below [11, 12]:

$$E_{MSE} = \frac{1}{N}\sum_{i=1}^{N}(y(i) - y_t(i))^2 \tag{29}$$

where $y(i)$ is the NN output, and $y_t(i)$ is the target data. In the training process of N2, the target of E_{MSE} is 0.001, and N equals 7075. Fig. 18 compares the trained data and actual output, and shows their differences for N2. We can see the controller can output the battery current effectively and the maximum error is less than 10A.

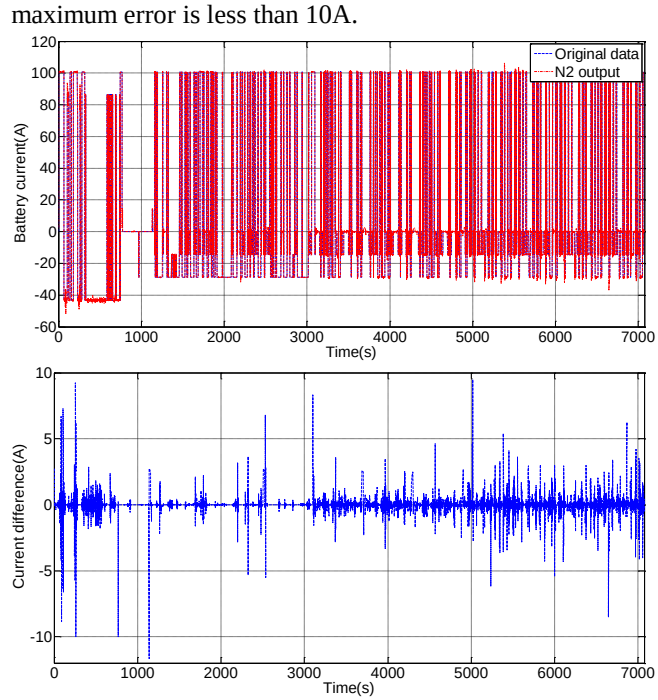

Fig. 18. The training result of N2.

This article has been accepted for publication in a future issue of this journal, but has not been fully edited. Content may change prior to final publication. Citation information: DOI 10.1109/TVT.2013.2287102, IEEE Transactions on Vehicular Technology

VI. Result Validation

According to the description of the controller in section V, when the trip length and trip duration are known in advance and the trip length is more than the AER calculated by the battery initial SOC, the controller will use N1 to output the battery current commands to manage the power distribution between ICE and battery. Usually the trip length and trip duration can be determined with the help of GPS / GIS or be estimated by experience. If the controller can not obtain them before the trip starts, it will use the battery to power the vehicle first until the battery SOC drops to a preset low-threshold (30%), and then use N2 to control the battery power.

A. Simulation with Knowing the Trip Length and Duration Precisely

Suppose the controller knows the trip length and duration precisely by GPS beforehand, we applied LA092 and REP05 drive cycles to validate the controller's performance.

The LA92 drive cycle's maximum speed is 67.30mph and its average speed is 24.61mph, it can represent the urban driving condition. The REP05 drive cycle can be mainly split into two parts, highway and urban driving, and its maximum speed is 80.20mph. These two drive cycles can include highway and urban driving conditions. Here, we select LA92 cycle repeating 4 and 6 times, and REP05 cycle repeating 2 and 3 times to make sure the trip lengths are more than the maximum AER. The beginning SOC is 100%, and the total driving distance is 39.24miles, 58.86miles, 40.08miles, and 60.12miles, and the time duration are 5740s, 8610s, 2800s, and 4200s, respectively. As presented in Table V, using the proposed controller, the fuel consumption can be reduced by 3.96%, 3.88%, 2.20%, and 2.79% with SOC correction included.

Fig. 19 compares the SOC variation when the two control algorithms are applied for four LA92 drive cycles, where we can see the SOC drops slower when the proposed controller is applied than that when the CD and CS algorithm is applied. Fig. 20 compares the engine operating efficiencies. We can see that the engine works more efficiently when the proposed controller is applied. This way, it can prove that the controller can improve the fuel economy.

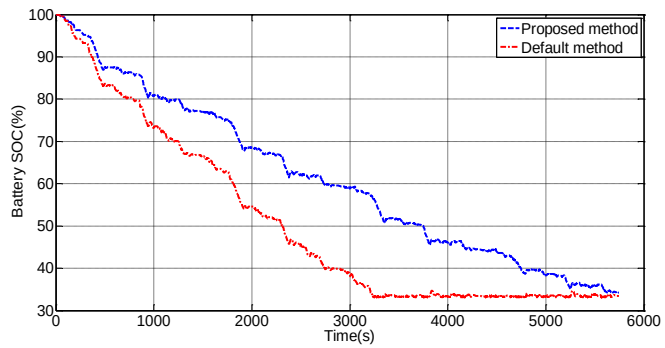

Fig. 19. Battery SOC comparison.

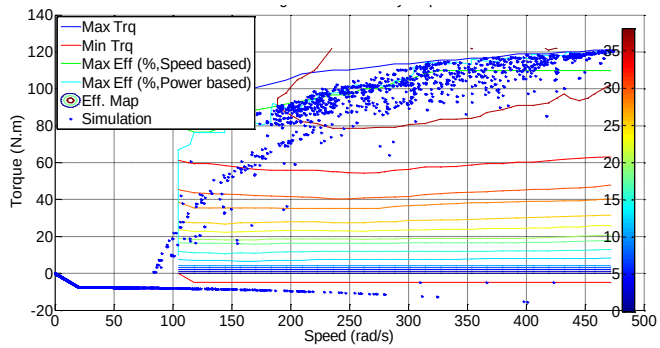

(a)

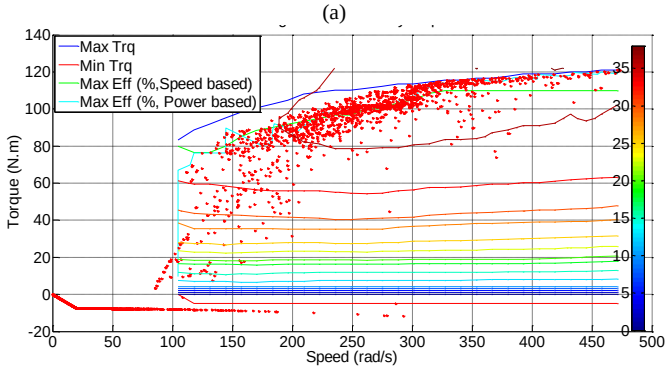

(b)

Fig. 20. Engine efficiencies comparison. (a). Default CS+CD algorithm. (b). The proposed controller.

Table V
Fuel Consumption Comparison

Drive cycle	Trip length (miles)	Trip duration (s)	Fuel consumption (Default algorithm) (kg)	Fuel consumption (Proposed algorithm) (kg)	Fuel savings (%)
4 LA92 cycles	39.24	5740	0.960	0.922	3.96
6 LA92 cycles	58.86	8610	1.959	1.883	3.88
2 REP05 cycles	40.08	2800	1.318	1.289	2.20
3 REP05 cycles	60.12	4200	2.473	2.404	2.79

B. Simulation with Estimation of the Trip Length and Duration

Usually we do not know the actual trip length and duration except with the help of GPS/GIS. However, we can generally estimate the trip distance by experience. The proposed algorithm is still feasible based on the estimated trip length and duration. In order to evaluate them, four consecutive Artemis drive cycles and seven New European drive cycles (NEDC) are simulated to validate the algorithm. With the default algorithm, the simulation result is shown in Table VI. The beginning SOC is 100%, the total fuel consumption is 0.722kg, and 0.882kg with the ending SOC of 31.36% and 31.53%, respectively.

This article has been accepted for publication in a future issue of this journal, but has not been fully edited. Content may change prior to final publication. Citation information: DOI 10.1109/TVT.2013.2287102, IEEE Transactions on Vehicular Technology

TABLE VI
THE FUEL CONSUMPTION COMPARISON AND SOC COMPARISON

Drive cycle	Length (miles)	Duration (s)	Fuel consumption (kg)	Ending SOC (%)
4 Artemis cycles	40.86	3924	0.722	31.36
7 NEDC cycles	47.88	8267	0.882	31.53

In order to validate the performance of the proposed algorithm, we considered four groups of parameters for trip length and duration for each drive cycle, which are shown in Table VII. Groups 1-4 parameters are for four Artemis cycles and groups 5-8 parameters are for seven NEDC cycles. Group 1 parameters are the actual trip parameters, and group 2 and group 3 parameters are smaller and larger than the actual parameters. In group 4, the trip length is larger, and the trip duration is shorter than the actual values. These three groups of parameters can reflect the differences of the estimated parameters. After simulation, the battery SOC curves based on different parameters are shown in Fig. 21. They are almost the same, and the ending SOC is 36.86%, 34.70%, 38.32%, and 34.03% respectively. From Table VII, with the SOC correction included, we can see that the proposed controller can save 4.02%, 5.12%, 5.82% and 3.74% of fuel consumption, compared with the default control algorithm. Table VII also compares the results for different trip length and duration when seven consectuive NEDC drive cycles are simulated. The ending SOC is 31.43%, 33.42%, 31.54%, and 34.62%, respectively, and the proposed controller can save 2.49%, 2.15%, 3.17% and 3.51% of fuel consumption, respectively. Therefore, the results show that the controller can improve the fuel economy based on the estimated trip length and duration.

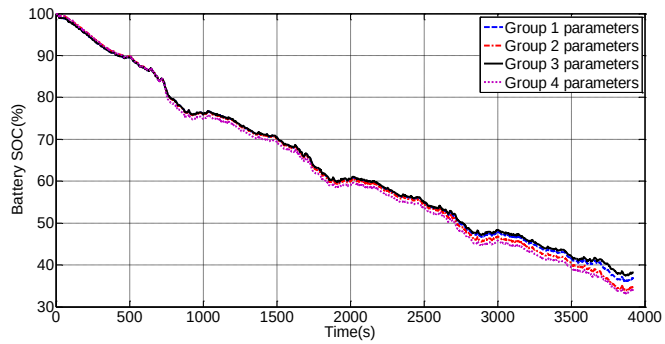

Fig. 21. SOC with different input parameters.

TABLE VII
THE FUEL CONSUMPTION COMPARISON AND SOC COMPARISON

Drive cycle	Groups	Estimated trip length (miles)	Estimated trip duration (s)	Fuel consumption (SOC corrected) (kg)	Ending SOC (%)	Fuel savings (%)
4 Artemis cycles	Group 1	40.86	3924	0.693	36.86	4.02
	Group 2	40.00	3600	0.685	34.70	5.12
	Group 3	42.00	4200	0.680	38.32	5.82
	Group 4	42.00	3600	0.695	34.03	3.74
7 NEDC cycles	Group 5	47.88	8267	0.860	31.43	2.49
	Group 6	50.00	8500	0.863	33.42	2.15
	Group 7	45.00	8000	0.854	31.54	3.17
	Group 8	45.00	8500	0.851	34.62	3.51

C. Simulation with Unknown Trip Length and Duration

Suppose we do not know any information about the trip length and duration. Based on the proposed controller, the vehicle uses all the stored electric energy first until the SOC drops to 30%, then N2 starts to work to output the battery current command to manage the power distribution. In order to validate the performance, three consecutive REP05 and four consecutive Artemis drive cycles are simulated.

The SOC variations based on the proposed controller and the default strategy are shown in Fig. 22 when three REP05 drive cycles are simulated. With the proposed controller, we can see the SOC first drops to 30%, which is the same as that when applying the default algorithm. Then the SOC maintains at the vicinity of 30%. Based on training of the optimal results obtained by DP method, N2 stores the optimal power distribution algorithm for different types of drive cycles, which makes the battery charge or discharge more frequently to ensure the engine works more efficiently. Fig. 22 shows that the SOC varies more obviously when the proposed controller is applied than that when the default controller is applied. The ending SOC based on the two algorithms is 32.5% and 30.08%. Table VIII lists the fuel consumptions based on different algorithms. The proposed algorithm can save 1.77% and 3.46% of fuel consumption with SOC correction included when three REP05 and four Artemis drive cycles are simulated. When the total driving distance and total driving duration are unknown, the proposed algorithm can still save fuel consumption compared with the default algorithm. However, the saving is less than that when the trip distance and duration is known, as presented in Table V and Table VII.

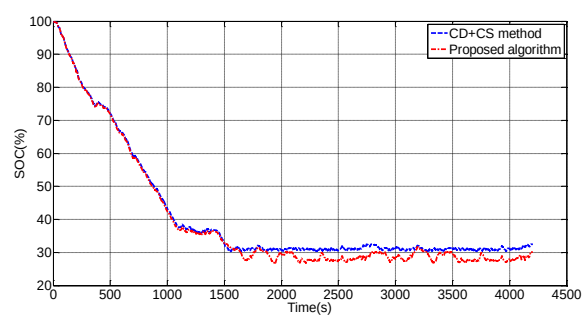

Fig. 22. SOC comparison.

This article has been accepted for publication in a future issue of this journal, but has not been fully edited. Content may change prior to final publication. Citation information: DOI 10.1109/TVT.2013.2287102, IEEE Transactions on Vehicular Technology

TABLE VIII
THE FUEL CONSUMPTION COMPARISON

Drive cycle	Length (miles)	Fuel consumption (Default algorithm) (kg)	Fuel consumption (Proposed algorithm) (kg)	Fuel savings (%)
3 REP05 cycles	60.12	2.433	2.390	1.77
4 Artemis cycles	40.86	0.722	0.697	3.46

VII. CONCLUSION

An effective online intelligent energy controller consisting of two NN control modules has been built to improve the fuel economy of a power-split PHEV. Based on whether the trip length and trip duration is known or unknown, the controller works differently to manage the energy distribution between the engine and the battery more intelligently, compared with the conventional CD and CS algorithm.

When the trip length and trip duration are known or can be estimated in advance, and if the trip length is more than the calculated AER, the controller will use N1 to calculate and generate the sub-optimal battery current commands to manage the power distribution between ICE and battery in real time based on vehicle speed, and other related parameters. If the trip length is less than the calculated AER, the vehicle will first use the battery to drive the vehicle. The simulation results validate the effectiveness of the controller.

If the controller cannot obtain the trip length and trip duration before the trip starts, the vehicle will be powered by battery first until the battery SOC drops to a preset low-threshold, and then the controller uses N2 to output the battery current commands. It can still improve the fuel economy.

In this paper, the controller is only validated by simulation. Besides, the controller does not consider the slope of the road, which can influence the vehicle driveline power. We also did not consider the battery aging and degradation issues, which can affect the AER as well as vehicle energy management. Our next step research will be carried out to consider them to improve the performance of the controller and validate the controller by experiment.

REFERENCES

[1] M. Ehsani, Y. Gao, and A. Emadi, *Modern Electric, Hybrid Electric, and Fuel Cell Vehicles: Fundamentals, Theory, and Design, Second Edition*: Taylor & Francis, 2009.

[2] V. Freyermuth, E. Fallas, A. Rousseau, and S. o. A. Engineers, *Comparison of Powertrain Configuration for Plug-in HEVs from a Fuel Economy Perspective*: SAE International, 2008.

[3] L. Guzzella and A. Sciarretta, *Vehicle Propulsion Systems: Introduction to Modeling and Optimization*: Springer, 2010.

[4] C. Mi, A. Masrur, and D. W. Gao, *Hybrid Electric Vehicles: Principles and Applications with Practical Perspectives*: Wiley, 2011.

[5] X. Zhang, *Power Systems: Vehicle Power Management: Modeling, Control and Optimization*: Springer London, 2011.

[6] C. C. Chan, A. Bouscayrol, and K. Chen, "Electric, Hybrid, and Fuel-Cell Vehicles: Architectures and Modeling," *Vehicular Technology, IEEE Transactions on,* vol. 59, pp. 589-598, 2010.

[7] P. B. Sharer, A. Rousseau, D. Karbowski, and S. Pagerit, "Plug-in Hybrid Electric Vehicle Control Strategy: Comparison between EV and Charge-Depleting Options," 2008.

[8] C. Zheng, F. Yuhong, and C. C. Mi, "State of Charge Estimation of Lithium-Ion Batteries in Electric Drive Vehicles Using Extended Kalman Filtering," *Vehicular Technology, IEEE Transactions on,* vol. 62, pp. 1020-1030, 2013.

[9] Z. Bingzhan, C. C. Mi, and Z. Mengyang, "Charge-Depleting Control Strategies and Fuel Optimization of Blended-Mode Plug-In Hybrid Electric Vehicles," *Vehicular Technology, IEEE Transactions on,* vol. 60, pp. 1516-1525, 2011.

[10] Z. Chen, C. C. Mi, R. Xiong, J. Xu, and C. You, "Energy management of a power-split plug-in hybrid electric vehicle based on genetic algorithm and quadratic programming," *Journal of Power Sources,* vol. 248, pp. 416-426, 2014.

[11] Y. L. Murphey, P. Jungme, L. Kiliaris, M. L. Kuang, M. A. Masrur, A. M. Phillips, and W. Qing, "Intelligent Hybrid Vehicle Power Control----Part II: Online Intelligent Energy Management," *Vehicular Technology, IEEE Transactions on,* vol. 62, pp. 69-79, 2013.

[12] Y. L. Murphey, P. Jungme, C. Zhihang, M. L. Kuang, M. A. Masrur, and A. M. Phillips, "Intelligent Hybrid Vehicle Power Control- Part I: Machine Learning of Optimal Vehicle Power," *Vehicular Technology, IEEE Transactions on,* vol. 61, pp. 3519-3530, 2012.

[13] C. Zheng and C. C. Mi, "An adaptive online energy management controller for power-split HEV based on Dynamic Programming and fuzzy logic," in *Vehicle Power and Propulsion Conference, 2009. VPPC '09. IEEE*, 2009, pp. 335-339.

[14] C. Zheng, Z. Xi, and C. C. Mi, "Slide Mode and Fuzzy Logic Based Powertrain Controller for the Energy Management and Battery Lifetime Extension of Series Hybrid Electric Vehicles," *Journal of Asian Electric Vehicles,* vol. 8, pp. 1425-1432, 2010.

[15] Z. Zhiguang, C. Mi, C. Zheng, A. Masrur, and Y. L. Murphey, "Power management of passive multi-source hybrid electric vehicle," in *Vehicle Power and Propulsion Conference (VPPC), 2011 IEEE*, 2011, pp. 1-4.

[16] K. Namwook, C. Sukwon, and P. Huei, "Optimal Control of Hybrid Electric Vehicles Based on Pontryagin's Minimum Principle," *Control Systems Technology, IEEE Transactions on,* vol. 19, pp. 1279-1287, 2011.

[17] X. Li, J. Li, L. Xu, M. Ouyang, X. Han, L. Lu, and C. Lin, "Online management of lithium-ion battery based on time-triggered controller area network for fuel-cell hybrid vehicle applications," *Journal of Power Sources,* vol. 195, pp. 3338-3343, 2010.

[18] H. Xi, T. Ying, and H. Xingui, "An Intelligent Multifeature Statistical Approach for the Discrimination of Driving Conditions of a Hybrid Electric Vehicle," *Intelligent Transportation Systems, IEEE Transactions on,* vol. 12, pp. 453-465, 2011.

[19] S. Stockar, V. Marano, M. Canova, G. Rizzoni, and L. Guzzella, "Energy-Optimal Control of Plug-in Hybrid Electric Vehicles for Real-World Driving Cycles," *Vehicular Technology, IEEE Transactions on,* vol. 60, pp. 2949-2962, 2011.

[20] M. Koot, J. T. B. A. Kessels, B. de Jager, W. P. M. H. Heemels, P. P. J. van den Bosch, and M. Steinbuch, "Energy management strategies for vehicular electric power systems," *Vehicular Technology, IEEE Transactions on,* vol. 54, pp. 771-782, 2005.

[21] J. T. B. A. Kessels, M. W. T. Koot, P. P. J. van den Bosch, and D. B. Kok, "Online Energy Management for Hybrid Electric Vehicles," *Vehicular Technology, IEEE Transactions on,* vol. 57, pp. 3428-3440, 2008.

[22] P. Jungme, C. Zhihang, L. Kiliaris, M. L. Kuang, M. A. Masrur, A. M. Phillips, and Y. L. Murphey, "Intelligent Vehicle Power Control Based on Machine Learning of Optimal Control Parameters and Prediction of Road Type and Traffic Congestion," *Vehicular Technology, IEEE Transactions on,* vol. 58, pp. 4741-4756, 2009.

[23] S. Ebbesen, P. Elbert, and L. Guzzella, "Battery State-of-Health Perceptive Energy Management for Hybrid Electric Vehicles," *Vehicular Technology, IEEE Transactions on,* vol. 61, pp. 2893-2900, 2012.

[24] S. G. Li, S. M. Sharkh, F. C. Walsh, and C. N. Zhang, "Energy and Battery Management of a Plug-In Series Hybrid Electric Vehicle Using Fuzzy Logic," *Vehicular Technology, IEEE Transactions on,* vol. 60, pp. 3571-3585, 2011.

This article has been accepted for publication in a future issue of this journal, but has not been fully edited. Content may change prior to final publication. Citation information: DOI 10.1109/TVT.2013.2287102, IEEE Transactions on Vehicular Technology

[25] H. Borhan, A. Vahidi, A. M. Phillips, M. L. Kuang, I. V. Kolmanovsky, and S. Di Cairano, "MPC-Based Energy Management of a Power-Split Hybrid Electric Vehicle," *Control Systems Technology, IEEE Transactions on,* vol. 20, pp. 593-603, 2012.

[26] W. Lei, E. G. Collins, Jr., and L. Hui, "Optimal Design and Real-Time Control for Energy Management in Electric Vehicles," *Vehicular Technology, IEEE Transactions on,* vol. 60, pp. 1419-1429, 2011.

[27] P. Pisu and G. Rizzoni, "A Comparative Study Of Supervisory Control Strategies for Hybrid Electric Vehicles," *Control Systems Technology, IEEE Transactions on,* vol. 15, pp. 506-518, 2007.

[28] Z. Zhou and C. Mi, "Power management of PHEV using quadratic programming," *International Journal of Electric and Hybrid Vehicles,* vol. 3, pp. 246-258, // 2011.

[29] G. Qiuming, L. Yaoyu, and P. Zhong-Ren, "Trip based optimal power management of plug-in hybrid electric vehicles using gas-kinetic traffic flow model," in *American Control Conference, 2008*, 2008, pp. 3225-3230.

[30] G. Qiuming, L. Yaoyu, and P. Zhong-Ren, "Trip-Based Optimal Power Management of Plug-in Hybrid Electric Vehicles," *Vehicular Technology, IEEE Transactions on,* vol. 57, pp. 3393-3401, 2008.

[31] Z. Menyang, Y. Yan, and C. C. Mi, "Analytical Approach for the Power Management of Blended-Mode Plug-In Hybrid Electric Vehicles," *Vehicular Technology, IEEE Transactions on,* vol. 61, pp. 1554-1566, 2012.

[32] S. J. Moura, H. K. Fathy, D. S. Callaway, and J. L. Stein, "A Stochastic Optimal Control Approach for Power Management in Plug-In Hybrid Electric Vehicles," *Control Systems Technology, IEEE Transactions on,* vol. 19, pp. 545-555, 2011.

[33] R. E. Bellman, *Dynamic programming*: Princeton University Press, 1957.

[34] S. C. Fang and S. Puthenpura, *Linear optimization and extensions: theory and algorithms*: Prentice Hall, 1993.

Zheng Chen (A'10–M'12) received the B.S.E.E. and M.S.E.E. degrees in electrical engineering and the Ph.D. degree in control science engineering from Northwestern Polytechnical University, Xi'an, China, in 2004, 2007, and 2012, respectively.

He is currently a post-doctor at the Department of electrical and computer engineering, University of Michigan- Dearborn. His research interests are in the areas of battery management system, battery status estimation, and energy management of hybrid electric vehicles. He was a visiting scholar at the University of Michigan-Dearborn from 2008 to 2011.

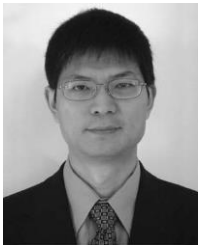

Chunting Chris Mi (S'00–A'01–M'01–SM'03 –F'12) received the B.S.E.E. and M.S.E.E. degrees from Northwestern Polytechnical University, Xi'an, China, and the Ph.D. degree from the University of Toronto, Toronto, ON, Canada, all in electrical engineering.

He is currently a Professor of electrical and computer engineering and the Director of the newly established Department of Energy-funded GATE Center for Electric Drive Transportation at the University of Michigan-Dearborn. Previously, he was an Electrical Engineer with General Electric Canada, Inc. He has been a Guest Editor for the International Journal of Power Electronics and Associate Editor for the Journal of Circuits, Systems, and Computers (2007–2009) and serves on the Editorial Board of the International Journal of Electric and Hybrid Vehicles and IET Electrical Systems in Transportation. He has conducted extensive research and published more than 100 articles. His research interests include electric drives, power electronics, electric machines, renewable-energy systems, and electrical and hybrid vehicles.

Dr. Mi was the Chair (2008–2009) and Vice Chair (2006–2007) of the IEEE Southeastern Michigan Section and the General Chair of the Fifth IEEE Vehicle Power and Propulsion Conference held in Dearborn on September 6–11, 2009. He has been an Associate Editor for the IEEE TRANSACTIONS ON VEHICULAR TECHNOLOGY, the IEEE TRANSACTIONS ON POWER ELECTRONICS LETTERS, and the IEEE TRANSACTIONS ON INDUSTRY APPLICATIONS, and a Senior Editor for the IEEE VEHICULAR TECHNOLOGY MAGAZINE. He received the "Distinguished Teaching Award" and "Distinguished Research Award" from the University of Michigan-Dearborn, the 2007 IEEE Region 4 "Outstanding Engineer Award," the "IEEE Southeastern Michigan Section Outstanding Professional Award," and the "SAE Environmental Excellence in Transportation Award.".

Jun Xu (S'13) received the B.S. degree in Mechanical Engineering from Xi'an Jiaotong University, Xi'an, Shaanxi, China, in 2009. He has been working toward the Ph.D. degree in Mechanical Engineering in the School of Mechanical Engineering since 2009.

From August 2011 to June 2013, he was a joint Ph.D. student founded by China Scholarship Council with the College of Electrical and Computer Science, University of Michigan, Dearborn, where he focused on battery management system for electric vehicles, hybrid electric vehicles and plug-in hybrid electric vehicles application. His research interests include design, analysis, testing and state estimation of battery system, including battery modeling, battery state estimation, battery balancing, etc.

Xianzhi Gong received the B.S. degree in Electrical Engineering and Automation from the Nanjing University of Aeronautics and Astronautics, Nanjing, China in 2009 and the M.S. degree from the Department of Electrical Engineering, University of New Haven, West Haven, CT, in 2011.

He is currently working toward the Ph.D. degree in Automotive Systems Engineering, University of Michigan-Dearborn, Dearborn, MI. His current research interests include battery management, renewable energy and power electronics.

Chenwen You received her B.S. degree in Electrical Engineering and Automation from the Huazhong University of Science and Technology, Wuhan, China in 2010. In 2012 she received her M.S. degree in Electrical Engineering from the Electrical and Computer Engineering Department, University of Michigan–Dearborn, where she is currently pursuing her Ph.D. degree in Automotive Systems Engineering. Her current research interests include power electronics, wireless charger, and power management in hybrid electric vehicles.